

Modeling of Precipitate Oxide and Sulfide Inclusions Formation in Liquid Steel

D. Didenchuk^a, D. Kalisz^{a*}

^a AGH University of Science and Technology, Faculty of Foundry Engineering, Krakow, Poland

*Corresponding author. E-mail address: dak@agh.edu.pl

Received 20.11.2015; accepted in revised form 29.12.2015

Abstract

The behaviour of non-metallic inclusions MnO, MnS, FeS, Al₂O₃, SiO₂, Y₂O₃, Y₂S₃ in liquid steel were modelled in commercial software FactSage. It allowed for calculating and designing diagrams of dependence of inclusions formation from the concentration of yttrium in determined limits of aluminium and oxygen. As a result, the influence of the increasing yttrium concentration on the precipitations of oxide and sulfide inclusions is observed. The behavior of precipitation the another analyzed oxides and sulfides is also observed in liquid steel, giving a full composition in non-metallic inclusions, formatted in specified conditions. The amounts of mass fractions of Y₂O₃ and Y₂S₃ are increasing at the growing Y in liquid steel, which shows the active formation of these inclusions.

Keywords: Yttrium; Non-metallic inclusions; Oxides; Sulfides; FactSage.

1. Introduction

Nowadays the qualitative requirements of construction materials have considerably raised, therefore modern metallurgists focus not only on the content of sulfur, phosphorus and gases in steel, but also on the content, form, distribution and size of non-metallic inclusions. The nonmetallic inclusions can be divided into sulphidic, oxidic and oxisulfidic. The latter are formed by dissolution of the remaining components and are a result of refining processes taking place beyond the furnace, i.e. mainly deoxidization and supplementation of the chemical composition. Such inclusions have a negative impact as they lower the strength and resistance to corrosion. Nonmetallic inclusions behave differently in local processes, significantly influence the origin of the centers of crystallization and formation of grains in steel. The perspective direction of modifying nonmetallic inclusions is the use of rare-earth metals and their combinations.

In this context authors of this paper carried out the modelling and further calculation of interaction of oxygen and sulfur with yttrium in metal. Yttrium actively reacts, firstly with oxygen and sulfur, forming complex oxide of type Y₂O₃ and Y₂S₃ sulfides of globular form.

The calculation of non-metallic inclusions in liquid steel was executed with the use of commercial software FACTSAGE [1]. Attention was also paid to the next formations of non-metallic inclusions in liquid steel: MnS, MnO, Al₂O₃, SiO₂, FeS.

For determining the parameters of interaction of inclusions with oxygen and sulfur it is necessary to know a constant of balance of deoxidization in metal [2-6].

The constant of balance for MnS inclusion in solid phase:

$$Mn + S = MnS \quad (1)$$

$$\log K = -8627/T + 4.745(s) \quad (2)$$

The constant of balance for MnO in liquid phase:

$$Mn + O = MnO \quad (3)$$

$$\log K = 16820/T - 7.79(l) \quad (4)$$

The constant of balance for Al₂O₃ in liquid phase:

$$2Al + 3O = Al_2O_3 \quad (5)$$

$$\log K = 64000/T - 20.57(l) \quad (6)$$

The constant of balance for SiO_2 inclusion in liquid and solid phases:



$$\log K = -30000/T + 11.40(s) \quad (8)$$

$$\log K = 30720/T - 11.78(l) \quad (9)$$

The constant of balance for FeS in liquid and solid phases:



$$\log K = 339/T + 2.57(l) \quad (11)$$

$$\log K = -1376/T + 3.74(s) \quad (12)$$

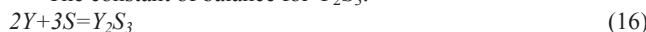
The constant of balance for Y_2O_3 inclusion in liquid and solid phases:



$$\lg K = -67028/T + 20.19(l) \quad (14)$$

$$\lg K = -71400/T + 21.81(s) \quad (15)$$

The constant of balance for Y_2S_3 :



$$\lg K = -61190/T + 23.10(s) \quad (17)$$

2. Modelling and calculation

For modelling the behavior of non-metallic inclusions we used another chemical composition of steel:

Table 1. The chemical composition of applied steel

C	Mn	Si	P	Cr	Ni	N	S
0.054	0.05	0.23	0.007	0.05	0.03	0.005	0.01

We were also interested in the use of components at the following limits: $\text{Y} = 0.02(0.01, 0.005) \%$, $\text{O} = 0.03(0.0005) \%$ and $\text{Al} = 0.02(0.015, 0.01, \text{and } 0.005) \%$.

Data that we got as a result of modelling allowed for the calculation and designing figures of dependence (Fig.1-8)

Fig.1-4. Diagrams of dependence of non-metallic inclusions (MnO , MnS , FeS , Al_2O_3 , SiO_2 , Y_2O_3 , Y_2S_3) formation from %Y in steel with high concentration of oxygen.

Fig.5-8. Diagrams of dependence of non-metallic inclusions (MnO , MnS , FeS , Al_2O_3 , SiO_2 , Y_2O_3 , Y_2S_3) formation from %Y in steel with low concentration of oxygen.

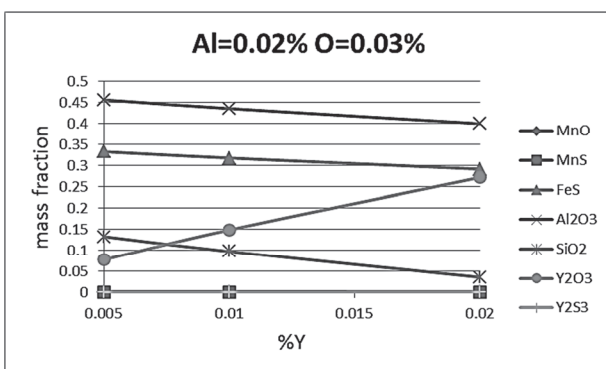


Fig. 1. Diagrams of dependence of non-metallic inclusions (MnO , MnS , FeS , Al_2O_3 , SiO_2 , Y_2O_3 , Y_2S_3) formation from %Y with $\text{Al}=0.02\%$ and $\text{O}=0.03\%$

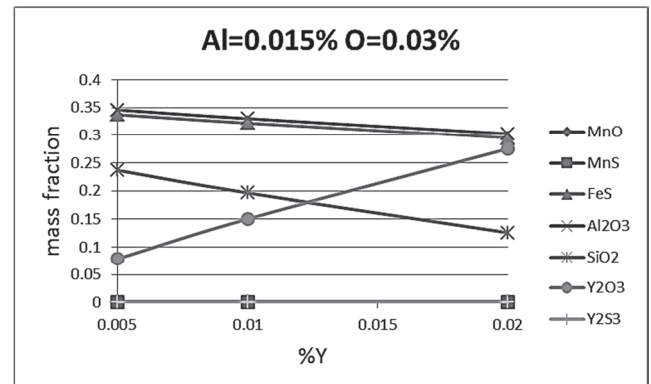


Fig. 2. Diagrams of dependence of non-metallic inclusions (MnO , MnS , FeS , Al_2O_3 , SiO_2 , Y_2O_3 , Y_2S_3) formation from %Y with $\text{Al}=0.015\%$ and $\text{O}=0.03\%$

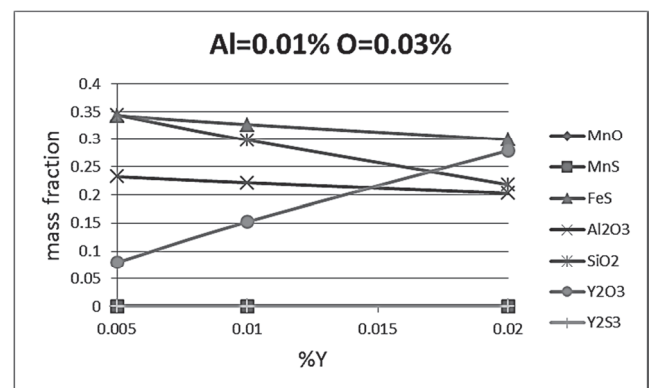


Fig. 3. Diagrams of dependence of non-metallic inclusions (MnO , MnS , FeS , Al_2O_3 , SiO_2 , Y_2O_3 , Y_2S_3) formation from %Y with $\text{Al}=0.01\%$ and $\text{O}=0.03\%$

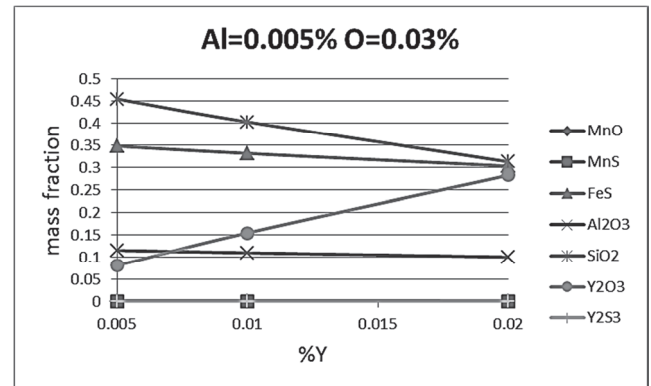


Fig. 4. Diagrams of dependence of non-metallic inclusions (MnO , MnS , FeS , Al_2O_3 , SiO_2 , Y_2O_3 , Y_2S_3) formation from %Y with $\text{Al}=0.005\%$ and $\text{O}=0.03\%$

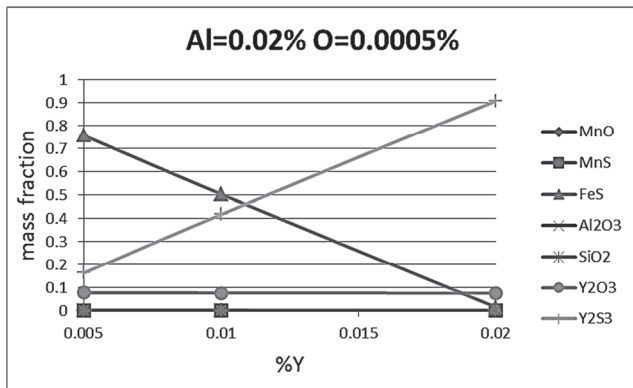


Fig. 5. Diagrams of dependence of non-metallic inclusions (MnO, MnS, FeS, Al₂O₃, SiO₂, Y₂O₃, Y₂S₃) formation from %Y with Al= 0.02% and O= 0.0005%

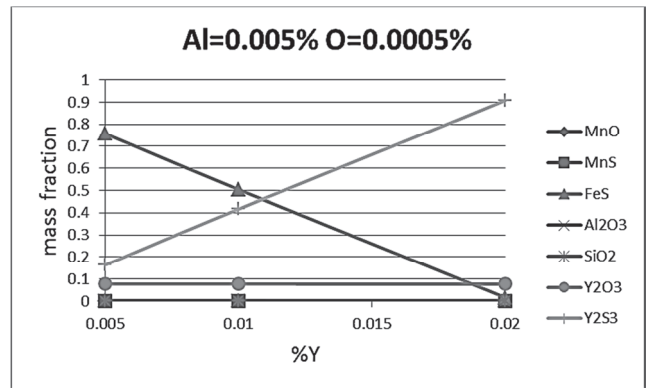


Fig. 8. Diagrams of dependence of non-metallic inclusions (MnO, MnS, FeS, Al₂O₃, SiO₂, Y₂O₃, Y₂S₃) formation from %Y with Al= 0.005% and O= 0.0005%

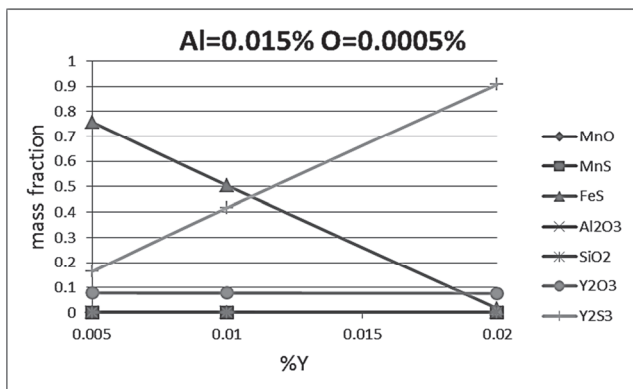


Fig. 6. Diagrams of dependence of non-metallic inclusions (MnO, MnS, FeS, Al₂O₃, SiO₂, Y₂O₃, Y₂S₃) formation from %Y with Al= 0.015% and O= 0.0005%

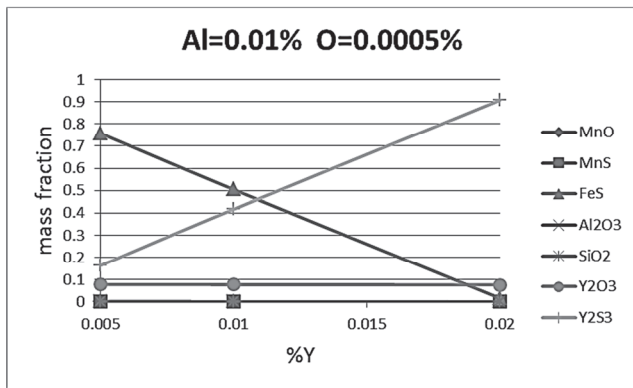


Fig. 7. Diagrams of dependence of non-metallic inclusions (MnO, MnS, FeS, Al₂O₃, SiO₂, Y₂O₃, Y₂S₃) formation from %Y with Al= 0.01% and O= 0.0005%

3. Results and discussion

For determining the precipitation of oxide and sulphide inclusions in liquid steel, the received data were modelled and calculated. The results of research are plots of non-metallic inclusions formation in a function of yttrium concentration. Therefore, we can observe the formation of inclusion for a different percent concentration of aluminium and oxygen in liquid steel. In figures 1-4 the O= 0.03%, and Al changes from 0.005% to 0.02%.

The analysis of the first diagram reveals that with the increasing yttrium concentration to 0.02% the mass fraction of Y₂O₃ actively formats. The diagram of Y₂O₃ is increasing from 0.07 mass fraction at Y= 0.005% to 0.3 at 0.02% of attached yttrium. The concentration of FeS is decreasing from 0.33 mass fraction at Y= 0.005% to 0.29 at Y= 0.02%. The Al₂O₃ inclusion is decreasing from 0.45 to 0.4. The SiO₂ diagram is decreasing from 0.15 at Y= 0.05% to 0.04 mass fraction.

On the fourth figure another situation is observed, i.e. with the decreasing concentration of aluminium from 0.02% to 0.005% the Al₂O₃ is equal to 0.012 at Y= 0.05% and 0.01 at Y= 0.02%. At the same time, the diagram of SiO₂ is equal to 0.45 at Y= 0.05% and 0.3 mass fraction at Y= 0.02%.

In figures 5-8 the concentration of oxygen is equal to 0.0005%, and aluminum limit are the same from 0.005% to 0.02%. In this case another behavior is observed.

First of all, the diagram of Y₂S₃ is increasing from 0.15 at Y= 0.005% to 0.9 at Y= 0.02%. The inclusion FeS is decreasing from 0.75 at Y= 0.005% to 0.0 mass fraction at 0.02% of yttrium. Concentration of Y₂O₃ is equal to 0.1 and does not change during increasing %Y. There are not formatting following oxide and sulfide inclusions: MnO, MnS, Al₂O₃, SiO₂.

4. Conclusions

The amount of mass fraction of Y₂O₃ is increasing at the increasing %Y in liquid steel which shows the active formation of

this oxide. On the other hand, the amount of other oxides (Al_2O_3 , SiO_2) in the analyzed steel is decreasing.

Also, the aluminum level has an influence on the formation of Al_2O_3 , SiO_2 inclusions, and when the concentration of Al is equal to 0.02% the mass fraction of Al_2O_3 stays in the range of 0.45-0.40. But when the concentration of Al is equal to 0.005% the mass fraction of SiO_2 is in the range of 0.45-0.35.

From the diagrams we can see that yttrium actively reacts with oxygen, because it has high deoxidization ability. And only then it reacts with sulphur, formatting the Y_2S_3 inclusion.

When the %O in liquid steel is low and consists of 0.0005% the mass fraction of yttrium is actively increasing from 0.18 to 0.9, instead of it the mass fraction of FeS is decreasing and at $\text{Y}=0.02\%$ is equal to 0. This shows us the high desulfurizing ability of yttrium in specified conditions of aluminium, oxygen and yttrium concentrations in liquid steel.

Acknowledgements

I express my strong gratitude to the UST – AGH, Faculty of Foundry Engineering for the opportunity to realize my research on this subject.

References

- [1] FactSage – commercial software
- [2] Liu, Z., Gu, K., Cail, K. (2002). *Mathematical Model of Sulfide Precipitation on Oxides during Solidification of Fe-Si Alloy*, ISIJ Int. 42.
- [3] Hallstedt, B. (1992). *Thermodynamic Assessment of the System $\text{MgO-Al}_2\text{O}_3$* . J. Am. Ceram. Soc. 75.
- [4] Tanahashi, M., Futura, N., Yamauchi, C., Fuisawa, T. (2001). *Phase Equilibria of the $\text{MnO-SiO}_2-\text{CrO}_x$ system at 1873 K under Controlled Oxygen Partial Pressure*. ISIJ Int. 41
- [5] Kobayashi, S. (1999). *Thermodynamic Fundamentals for Alumina Content Control of Oxide Inclusions in Mn-Si Deoxidation of Molten Steel*. ISIJ Int. 38.
- [6] Mikhailov, G.G., Makrovets, L.A. (2014). *Thermodynamic simulation of phase equilibria with oxide systems containing rare earth-metals, Phase diagrams of oxide systems with Y_2O_3* . Bulletin of South Ural State University 5-10.
- [7] Wypantowicz, J., Podorska, D. (2006) *Control of chemical composition of oxide-sulfide inclusions during deoxidization of steel*. Metallurgy-Metallurgical Engineering News 3, 91-96.
- [8] Iwanciw, J., Podorska, D., Wypantowicz, J. (2011). *Modeling of oxide precipitates chemical composition during steel deoxidization*. Archives of Metallurgy and Materials 56(4), 999-1005 DOI: 10.2478/v10172-011-0110-0.
- [9] Iwanciw, J., Podorska, D., Wypantowicz, J. (2011) *Simulation of oxygen and nitrogen removal from steel by means of titanium and aluminium*. Archives of Metallurgy and Materials 56(3), 635-614 DOI: 10.2478/v10172-011-0069-x.
- [10] Podorska, D., Drozdz, P., Falkus, J., Wypantowicz, J. (2006). *Calculation of oxide inclusions composition in the steel deoxidized with Mn, Si, Al and Ti*. Archives of Metallurgy and Materials 51, 581-586.
- [11] Iwanciw, J., Podorska, D., Wypantowicz, J. (2010). *Zechowanie dodatków wytopowych w procesie rafinacji stali*. Metallurgy-Metallurgical Engineering News (Hutnik) 77(4), 132-139.
- [12] Kalisz, D. (2012). *Modelowanie procesów rafinacji i wprowadzania azotu w stalach elektrochemicznych*. Wydawnictwo naukowe AKAPIT 1, 120.